

The Evaluation of the Cylindrical Accuracy in Bore Honing of EN-GJL-250 Lamellar Cast Iron

István Sztankovics^{1*}

¹ *Institute of Manufacturing Science, University of Miskolc
Egyetemváros, Miskolc, H-3515, HUNGARY*

*Corresponding Author: istvan.sztankovics@uni-miskolc.hu

DOI: <https://doi.org/10.30880/ijie.2025.17.01.011>

Article Info

Received: 18 August 2024

Accepted: 6 December 2024

Available online: 30 April 2025

Keywords

Cylindricity, factorial design, honing, shape accuracy

Abstract

The study of the different parameters, which describe the shape accuracy of the machined parts is important on functionally significant surfaces. The cylindrical accuracy is an essential characteristic of the machined bores of internal combustion engine blocks. The aim of the ongoing study is to explore the relationship between the shape error of the produced inner cylindrical surfaces and the setting parameters in honing. The results contribute to a wider understanding of the achievable precision of the examined finishing process by examining the relationships that have not been determined so far. In this paper, four parameters describing the cylindrical error after the honing procedure are analysed on EN-GJL-250 lamellar cast iron workpieces. The 23 factorial design is applied in the planning of experiments. Two levels of grain size, feed rate and pressure between the workpiece and the honing tool were chosen for the comprehensive analysis of the internal cylindrical honing process. The values of cylindricity, the valley maximum departure, the peak maximum departure and the cylinder taper are measured by the application of a Talyrond 365 accuracy measuring equipment. Equations were determined for the calculation of the studied parameters according to the full factorial design method. The results were evaluated in three steps: first the main effect of the process parameters are determined, then the presented equations are validated through control experiments. Finally, the detailed analysis of the results showed the alteration of the cylindrical correctness in function of the different parameters.

1. Introduction

In the production planning of different kinds of parts, the responsible engineers must pay attention to meet the prescribed quality requirements of the produced workpieces, while reaching productivity levels as high as possible. Efficiency and environmental impact are also some important factors, which must be taken into consideration. The designers could prescribe various quality requirements, which are needed and important for the proper functional behavior of the product. The machined surface quality is one aspect, while the accuracy of the product is also essential. The latter can be defined for three kinds of characteristics for the workpiece: dimensional accuracy, position accuracy and shape accuracy. In this paper, one attribute of the shape accuracy is studied, due to its importance in the working conditions of a given part. The different kinds of shape accuracy parameters are important for those surfaces which are contacting during the regular operation of the assembled parts. For example, Shen and Lu showed that the form deviations of the fitted parts affect the contact forces, thus the influences of form deviations considering spatial distribution characteristics and local surface deformations cannot be ignored [1].

This is an open access article under the CC BY-NC-SA 4.0 license.



There are many types of parameters, which can be define the geometrical accuracy of a produced workpiece, from which the study of the cylindricity of different cylindrical parts is widespread many decades ago [2]. The definition of the cylindrical error is shown in Figure 1. Ideally, the machined workpiece should be a perfect cylinder. However, due to different effects occurring in machining, the realized surface takes the form of a noncylindrical geometric shape. The real surface can be enclosed between two concentric cylindrical surfaces, where the radial deviation between these two will mean the cylindrical error of the part (Figure 1.a). On the mechanical drawings, the maximum tolerance value of this radial deviation can be given with the proper geometrical error specification (Figure 1.b). In short, the cylindricity requirement specifies how accurately circular and straight a target cylinder is, where the value represents any distortion in a cylinder [4].

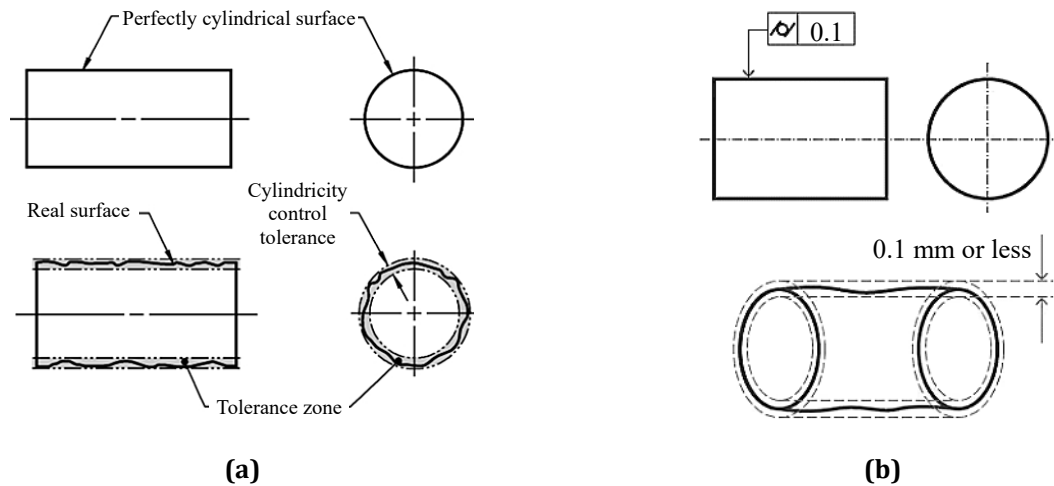


Fig. 1 Description: (a) Cylindrical error tolerance zone [3]; (b) Indication on mechanical drawings [4]

There are various fields in the manufacturing science, where the study of the cylindrical error is important. Umarov et al. analysed the shape error of machined holes by drilling and the relations between the error, the ratio of angular velocities and the frequency of rotation are determined [5]. Motorcu and Ekici are determined the order of influence on the hole roundness (a related shape error parameter) of the cutting speed, cutting tool geometry, feed rate in drilling of difficult-to-machine materials [6]. Machno et al. applied a factorial design plan to analyse the radial overcut and cylindricity in electrical discharge machining of a titanium alloy [7]. In their study, the evaluation of hole quality is complemented by the analysis of the material removal rate. Felhő et al. also showed the effectiveness of applying a properly planned design approach in their work [8]. Varga and Ferencsik analysed various parameters describing the cylindricity error in their study of high and low temperature storage tested alternator stators [9]. Nagy and Varga studied cylindrical accuracy among other quality parameters in turning of shaft with differently applied coolant and lubricants [10]. Varga et al. also studied the achievable shape accuracy in diamond burnishing of cylindrical parts [11]. They studied by the factorial experiment design method how the different process- and postprocessing influence the improvement in shape accuracy (namely circularity error and deviation of cylindricity) in the case of cylindrical test specimens. The improvement possibilities of the circularity are showed.

The most important parts in the automotive industry are the components of the engine block. There are many kinds of research and developments ongoing, which intend to improve the efficiency of internal combustion engines. An approach could be the improvement of the applied lubrication materials. Kuti et al. showed that significant amount of fatigue wear, including some deep abrasive grooves, is visible on the contacting surfaces and both wear mechanisms could be traced back to lubrication anomalies. The proper selection of engine oils is showed in their work [12]. Another field in the improvement of engines is the development of proper finishing procedures. Karpuschewski et al. proved, that the final honing step can be substituted by burnishing with an improved tribological load-carrying capacity [13]. However, deep valleys and flattened peaks are essential characteristics of the finished cylinder bore surface, which is known as the plateau surface. This can be achieved by the application of the honing procedure, which is the subject of much research nowadays. The results of the study of Sadizade et al. revealed that, by replacing a three-stage honing process with an optimized two-stage process without sacrificing surface qualities, a threefold reduction in the whole honing process time can be also achieved [14]. Mawandiya et al. carried out a performance optimization in the honing machining process in their work using the principle of cycle time study and balancing of the stations [15]. Buj-Corral et al. carried out experimental finishing honing tests and they found that the combination of high grain size, high density, high pressure, high tangential speed and high linear speed is not recommended, because it provides high roughness,

high cylindrical error and high tool wear [16]. Kundrák et al. developed models of the diamond-bearing layer of a wheel with different grain concentrations [17]. Based on the results of dynamic modelling, the dependences of the destruction volumes of diamond grains, bonds, and the processed material on the concentration of diamond in the grinding wheel and the type of the processed material were obtained which is essential in abrasive machining. Baron et al. also showed that for a honing process of grey cast iron the designed honing stones with defined cutting edges enable higher material removal rates by lower workpiece roughness compared to conventional tools [18]. Very uniform and reproducible workpiece roughness and cutting paths were achieved in grey cast iron. Engines blocks are usually made of grey cast irons. The lamellar structured variant is harder and in the same time become more brittle [19], which characteristic must take into consideration in the process planning. The fatigue behaviour and lifetime can be characterized by different type of test, which are described by Germann et al. [20] They showed, that the EN-GJL-250 material grade has the proper attributes for an engine block, however the machinability of this material is moderately good, the operation planning must be carried out carefully.

In summary, the analysis of the cylindrical accuracy is important in the finish machining of bore holes in the engine block, which often carried out by honing. The aim of the ongoing research is to contribute to the deeper understanding of the achievable shape accuracy as function of the setting parameters in honing. In this paper, a study is carried out to analyse the effect of the pressure, grain size and feed rate on the different parameters describing the cylindrical error. The determination of the effect of these parameters gives novel information for the production planning of the honing process when an EN-GJL-250 material is applied and it helps in the improvement of the honing process. The 2^k full factorial experimental design method was applied to select the analysed values of process parameters. The values of Cylindricity ($CYLt$), the valley maximum departure ($CYLv$), the peak maximum departure ($CYLp$) and the cylinder taper ($CYLt$) are measured and studied according to the expected functional behaviour of the machined surface.

2. Methods and Conditions

In this paper, the cylindrical accuracy of bore honed sleeves is studied. The evaluation is carried out on the basis of the realized experiments. Theoretical equations were also determined by the application of the 2^k full factorial design method. The experimental conditions and the analyzed parameters are detailed in the following.

The bore honing machining of the workpieces is carried out on a WMW 270/700 machine tool, which was provided by Belcord Kft. located in Eger, Hungary (their assistance is greatly appreciated). Sleeves with 192 mm bore length and 88 mm inner diameter are honed during the experiments, which geometry is frequently used by the industrial partner. The material of the workpieces was chosen to EN-GJL-250 material, which is a lamellar cast iron grade. Some of the nominal mechanical properties of the material are 250 MPa Tensile Strength, 210 HB Hardness, 110 kN/mm² Elasticity modulus, 950 MPa Compressive Strength. The honing tool has six slots with 60° from each other, where the honing stones with 120 mm length and 10 mm × 10 mm square cross-section are clamped. The chosen abrasive materials were Al₂O₃ grains in a synthetic resin binder with a dense structure. Tools with rougher and finer grain sizes are applied during the cutting experiments.

Three variable parameters were adjusted during the experiments. The two-level variation of the 3 parameters resulted in 8 experimental setups, which are presented in Table 1. Two different sizes of grains are chosen: the finer honing tool had 45 μm average grain size (d_k) which corresponds to the size code of 240; the rougher honing tool had 190 μm average grain size which corresponds to the size code of 80.

Table 1 Experimental setups

Setup	Selected factors			Design matrix		
	p [bar]	v_f [mm/rev]	d_k [μm]	p' [-]	v_f' [-]	d_k' [-]
1	7	25	45	-1	-1	-1
2	13	25	45	1	-1	-1
3	7	75	45	-1	1	-1
4	13	75	45	1	1	-1
5	7	25	190	-1	-1	1
6	13	25	190	1	-1	1
7	7	75	190	-1	1	1
8	13	75	190	1	1	1

The applied pressure (p) by the honing tool on the inner cylindrical surface of the workpiece was set to 7 bar and 13 bar and the axial feed of the honing stone during one rotation of the tool (v_f) was set to 25 mm/rev and 75 mm/rev. The cutting speed (v_c) was constant during the experiments, and it was set to 200 m/min. These values

were chosen according to the recommendations and experience of the industrial partner. The exact values of the selected factors are presented in Table 1, additionally the resulted design matrix is displayed which was determined according to the 2^k full factorial design method. The experiments are carried out once in this preliminary study, the reliability of the results is tested by further experiments which will be described later.

Shape error measurements were carried out after the cutting experiments on a Talyrond 365 accuracy measuring equipment. The setup parameters in the program were chosen according to the standard and earlier practical experience.

An important detail is the proper choice of the applied reference cylinder. In this study, the Least Squares Cylinder (*LSCY*) is used. This is the most stable reference cylinder and hence it is the most used. Importantly, it uses the axis that is used when centring and levelling a component to the rotational datum. Consideration of the other reference cylinders will reveal that their axes can be swayed by extreme data [21]. The measurements were made in seven planes with 10 mm separation between each, therefore a cylinder with 60 mm axial length is measured in one run. Each workpiece is measured twice from both sides, and the measurement results will be averaged. This consideration and setup are made due to the limitations of the workpiece geometry and the measuring device. The analysed parameters were the following (ISO 12180-1) [21]:

- *CYLt* – Cylindricity, the min. radial separation of two cylinders, coaxial with the fitted reference axis [μm]
- *CYLv* – the valley maximum departure from the reference cylinder into the material of the workpiece [μm]
- *CYLp* – the peak maximum departure from the fitted reference [μm]
- *CYLtt* – Cylinder Taper, the cylinder parallelism or the taper in the component [μm]

The results were used to determine equations for the better understanding of the honing process. These were worked out using the form in Equation 1 according to the 2³ full factorial design method. The *y* is the expressed dependent value and *k_i* are the coefficients describing the effect of the different factors on the dependent value. The independent variables are the pressure (*p*), feed (*v_f*) and average grain size (*d_k*). The analysis and data approximations were performed in the Maplesoft Maple 16 mathematical software. This program uses functions which are capable of the calculation and evaluation of the formulas used by the full factorial design method.

$$y(p, v_f, d_k) = k_0 + k_1p + k_2v_f + k_3d_k + k_{12}pv_f + k_{13}pd_k + k_{23}v_fd_k + k_{123}pv_fd_k \tag{1}$$

The fit will be clearly appropriate in the points corresponding to the 8 experimental setups. Further experiments should be made and evaluated in the middle points, to validate the results. However, the changing of the grain size was not possible during the experiments due to the available tools. Therefore, two more experiments (1-1 with each honing tool) are carried out in order to test the goodness of the determined equations with a feed rate of 50 mm/min and pressure of 10 bar. The details of the resulted validation setups (V1 and V2) are summarized in Table 2.

Table 2 Validation setups

Setup	Selected factors		
	<i>p</i> [bar]	<i>v_f</i> [mm/rev]	<i>d_k</i> [μm]
V1	10	50	45
V2	10	50	190

3. Experimental Results

After the machining of the sleeves, the designed measurements were carried out. Each workpiece was measured twice from both sides due to the length of the machined workpiece and the limitation in length of the device arm. The machine registered a roundness profile in 7 planes 10 mm from each other, and these were linked together to draw the cylindrical profile.

The software of the measuring device determined the above described cylindricity error parameters. The results of the two separate measurements of each bore are presented in Table 3. The calculated averages are also given in the table. The exact values of the total error (*CYLt*), valley depth (*CYLv*), peak departure (*CYLp*) and cylinder taper (*CYLtt*) give one comparison possibility, however it is also important to analyse the distribution of the geometric inaccuracy. Due to the importance of the distribution of the error, the ratio of the peak deviation and the cylindricity (*CYLp / CYLt*) as well as the ratio of the valley departure and the cylindricity (*CYLv / CYLt*) are also calculated, which results are shown in Table 4. These ratios allow a deeper understanding of the shape error characteristic of the machined surface, hence the inclusion in this study.

The values given in Table 3 are further evaluated according to the principles of the full factorial design plan and equations are determined in the form of Equation 1. These are used primary in the evaluation of the measured

data, as the equations and the graphs which can be drawn using these help the understanding the characteristic effect of the pressure, feed rate and average grain size in the studied parameter ranges.

The calculation formulas for $CYLp$, $CYLv$, and $CYLt$ are shown in Equation 2-4. The cylinder taper can be determined using Equation 5. The ratios of the peak departure and the cylindricity error; and the valley departure and the cylindricity error are studied with Equation 6-7.

$$CYLp(p, v_f, d_k) = -1.31 + 0.72p + 0.28v_f + 0.037d_k - 0.017pv_f - 0.0039pd_k - 1.62 \cdot 10^{-3}v_f d_k + 1.4 \cdot 10^{-4}pv_f d_k \quad (2)$$

$$CYLv(p, v_f, d_k) = -5.23 + 1.07p + 0.09v_f + 0.028d_k - 8.6 \cdot 10^{-3}pv_f - 1.7 \cdot 10^{-3}pd_k - 1.77 \cdot 10^{-4}v_f d_k - 9.8 \cdot 10^{-6}pv_f d_k \quad (3)$$

$$CYLt(p, v_f, d_k) = -6.54 + 1.79p + 0.37v_f + 0.064d_k - 0.025pv_f - 0.0056pd_k - 0.0018v_f d_k + 1.32 \cdot 10^{-4}pv_f d_k \quad (4)$$

$$CYLtt(p, v_f, d_k) = -2.34 + 0.83p + 0.44v_f + 0.024d_k - 0.037pv_f - 0.0013pd_k - 6.93 \cdot 10^{-4}v_f d_k + 5.22 \cdot 10^{-5}pv_f d_k \quad (5)$$

$$CYLv/CYLt(p, v_f, d_k) = +0.1637 + 0.028p - 0.0019v_f + 0.0011d_k - 4.02 \cdot 10^{-5}pv_f - 6.33 \cdot 10^{-5}pd_k - 1.586 \cdot 10^{-5}v_f d_k + 2.069 \cdot 10^{-6}pv_f d_k \quad (6)$$

$$CYLp/CYLt(p, v_f, d_k) = +0.8363 - 0.028p + 0.0019v_f - 0.0011d_k + 4.02 \cdot 10^{-5}pv_f + 6.33 \cdot 10^{-5}pd_k - 1.586 \cdot 10^{-5}v_f d_k + 2.069 \cdot 10^{-6}pv_f d_k \quad (7)$$

Table 3 Experimental results

Setup	Data set	$CYLp$ [μm]	$CYLv$ [μm]	$CYLt$ [μm]	$CYLtt$ [μm]
1	1	10.10	3.56	13.66	9.78
	2	5.18	3.33	8.51	7.16
	Average	7.64	3.45	11.09	8.47
2	1	11.22	6.46	17.68	6.97
	2	7.52	9.58	17.09	8.90
	Average	9.37	8.02	17.39	7.94
3	1	16.60	6.08	22.68	25.26
	2	12.68	2.71	15.39	8.65
	Average	14.64	4.40	19.04	16.96
4	1	11.49	9.65	21.14	5.42
	2	15.10	2.83	17.93	6.55
	Average	13.30	6.24	19.54	5.99
5	1	6.52	5.56	12.08	8.88
	2	6.88	4.28	11.16	10.18
	Average	6.70	4.92	11.62	9.53
6	1	7.34	12.13	19.47	10.61
	2	8.91	3.47	12.38	7.44
	Average	8.13	7.80	15.93	9.03
7	1	12.54	4.90	17.44	17.64
	2	5.73	3.27	8.99	13.64
	Average	9.14	4.09	13.22	15.64
8	1	13.43	4.83	18.25	8.07
	2	13.90	2.78	16.68	5.87
	Average	13.67	3.81	17.47	6.97

Table 4 Calculation of the ratio parameters

Setup	1	2	3	4	5	6	7	8
$CYLp / CYLt$ [-]	0.67	0.54	0.78	0.69	0.58	0.55	0.68	0.78
$CYLv / CYLt$ [-]	0.33	0.46	0.22	0.31	0.42	0.45	0.32	0.22

4. Discussion

The specification of the applied methods and equipment and the presentation of the measured results and calculated equations are followed by the evaluation of the obtained data. The results in Table 3 show a relatively low deviation between the measured data and their averages. However, in some cases of the 32 results, there is a noticeable difference between the two measurement results. This can be explained by the fact that there are random errors as well, which contributes to the actual shape error of the machined bores. In this study, the overall effect of the selected setting parameters is studied. Therefore, these results fulfill the task in order to achieve the determined goal. The results can be investigated to establish the relations between the process parameters and the shape accuracy values. The analysis is done in three steps by the processing of the measurements and worked out equations.

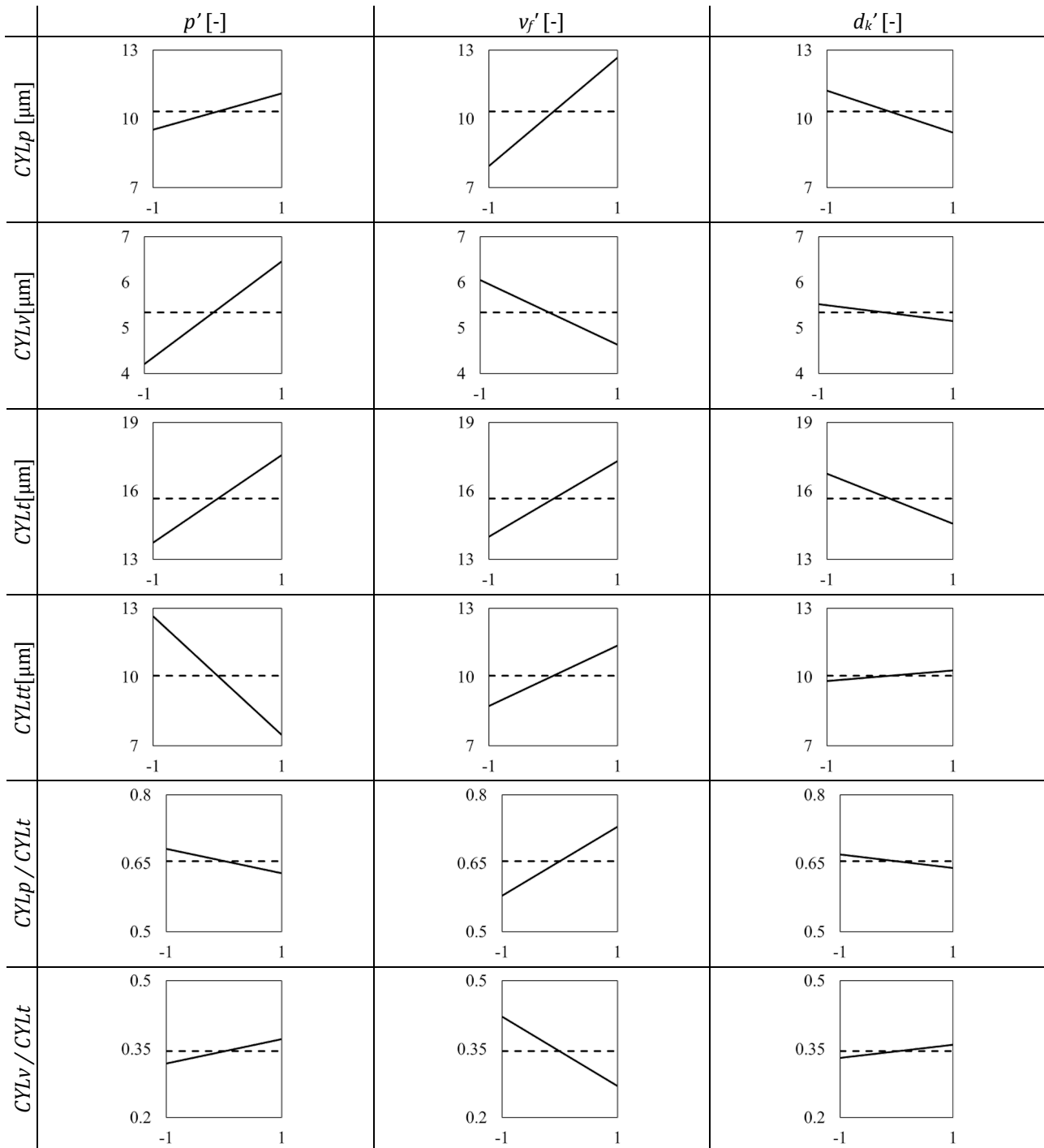


Fig. 2 Main effect plots of p, v_f, d_k on the studied parameters

Firstly, the main effect plots of the studied varied technological parameters on the measured cylinder accuracy parameters are drawn and analyzed. Secondly, the determined formulas are used to calculate the theoretical values of the accuracy parameters in the middle points of the analyzed ranges, which are compared with the experimental results collected in machining with the technological parameters presented in Table 2. Lastly, surface diagrams are drawn based on Equation 2-7, which are evaluated to show the detailed effect of the pressure, feed rate, and average grain size on the studied cylindricity parameters.

4.1 Evaluation of the Main Effects

Main effect plots were drawn for the initial evaluation of the effect of the three studied parameter. Each analysed cylinder accuracy parameters are studied separately as described below. First the mean value of the averaged values is calculated, which are represented by a dashed line. Then two mean values were calculated again for the three studied cutting parameters, where the results are separated according to the lower (-1) and upper (1) limit of p , v_f and d_k . These two averages are linked with a continuous line. The direction and gradient of the slope of these lines describe the main effect of the cutting parameter on the studied cylindricity parameters. The resulted main effect plots of the different cutting parameters on the studied cylinder accuracy parameters can be seen in Figure 2.

The increasing pressure has a high impact on the valley depth, resulting in an almost 1.5-fold increase. As we increase the pressure, the abrasive grains can penetrate the workpiece material deeper, thus explaining the observed effect. However, the increased pressure has a lesser effect on the peak height. The relatively small increase can be explained by the displacement of the reference cylinder during the measurements due to the changing profile of the generated marks. Overall, higher pressure resulted in higher cylindricity in the studied region. The feed rate has a more complex effect on these three shape error values. As the feed rate increases, the peak height significantly increases while the valley depth lightly decreases. With the honing stones moving faster, there is less time available to wear down the top parts of the workpiece material and to deepen the machined profile. The combined effect results in an increasing overall cylindricity error. The average size of the grains has a decreasing effect on the $CYLp$, $CYLv$, and $CYLt$ parameters. As the size of the abrasive particles become higher, the contact length between these and the workpiece material increases due to the higher average radius of the micro-edges doing the cutting. This leads to producing wider but shallower micro-scratches on the workpiece by the abrasive grains, which results in the overall decrease in the analysed cylindricity errors. The cylinder taper is highly affected by the applied pressure in the studied range, where higher pressure tends to lower significantly the value. The feed rate has a smaller increasing effect on the $CYLtt$, while the grain size has almost zero effect. The last two rows of Figure 2 present the main effect of the analysed setup parameters on the studied ratio parameters. It can be concluded by the examination of the graphs, that increasing the feed slightly decreases the peak rate from the cylindricity and slightly increases the valley rate. The same directional change can be expected by applying higher grain sizes in the tools. However, the overall main effect of these setup parameters is almost negligible. Although, the increasing feed rate has a greater impact on the ratio parameters. Higher feed rate results higher rated peak deviations, and lower valley errors.

4.2 Validation of the Determined Equations

The study continues by the validation of the determined equations, which is presented in Table 5. The basic characteristic of the full factorial design method is the changing accuracy of the deducted equations in the analysed range. Since it approximates the formulas based on the experimental setups, the accuracy will be higher near the corners of the range, and it could become less accurate as we move away from these points. Therefore, higher inaccuracy can be expected in the middle of the analysed range.

Table 5 Results of the validation measurements

Setup	Data set	$CYLp$ [μm]	$CYLv$ [μm]	$CYLt$ [μm]	$CYLtt$ [μm]
V1	Measure 1	9.49	6.83	16.32	12.20
	Measure 2	9.07	4.70	13.77	8.89
	Average	9.28	5.77	15.05	10.55
	Theoretical	9.41	5.15	14.56	10.28
	Difference	1.4%	-12.0%	-3.3%	-2.6%
V2	Measure 1	10.36	9.75	20.11	16.11
	Measure 2	9.56	2.60	12.16	6.81
	Average	9.96	6.18	16.14	11.46

Theoretical	11.24	5.52	16.76	9.83
Difference	11.4%	-11.9%	3.8%	-16.6%

However, the grain size cannot be changed (since the applied two tool variants are given), therefore two validation experiments are carried out. Table 5 shows the results of the two measurements of the 4 analysed shape error parameters and their averages. It also shows the theoretical value of each parameter, which are calculated by the application of Equation 2-5. Finally, the difference from the averages and the theoretical values are also presented. It can be seen that the difference is between -3.3% and 3.8% in four cases. The calculations have a difference between -12.0% and 11.4% for 3 cases and in one case a -16.6% difference can be observed. Overall, it can be concluded, that the determined equations can be applied to approximate the expected shape error in different points of the analysed setup range.

4.3 Detailed Analysis of the Results and the Determined Equations

The final part of the paper is the detailed analysis of the results by the application of the determined equations, which are visualized in Figure 3 and 4. These show that the resulted surface plots fit almost perfectly in those points where the experiments were carried out. This is caused by the fact that the full factorial design method fits the quadratic function at these points. The showed surface plots present the alteration of the analysed parameters between these points. The carried-out validation proved, that the approximation is good in the middle points of the analysed ranges as well. Figure 3 and 4 shows the results of the experiments and the determined equations in two plots for each parameter as function of the feed rate and pressure on the two separate levels of the grain size. It is possible to visualize the result in one graph, where the measurement results could be represented by colour in an extended 3D diagram with axes of d_k , v_f and p . However, when a machining procedure is applied, usually the cutting tools are given or not easily changeable. Therefore, it is enough to present the resulted surface diagrams in separate plot-pairs.

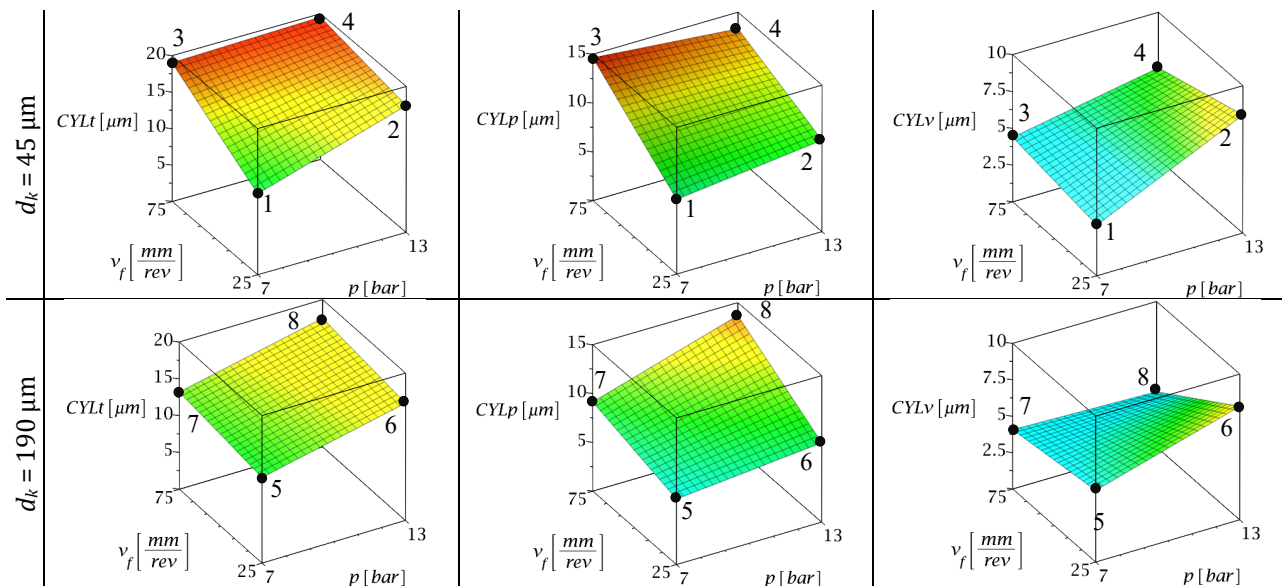


Fig. 3 Alteration of the CYLt, CYLp and CYLv values in the studied range (the setup numbers are shown)

Figure 3 presents the determined surface plots on the two different grain size levels for the cylindricity error, peak maximum departure and valley maximum departure parameters. The grain size has an overall lowering effect on the cylindricity, if 75 mm/rev feed rate is applied: a 4-fold increase in d_k results in a nearly 20% decrease in this shape error parameter. However, the grain size has a smaller decreasing effect, when 25 mm/rev feed rate is set. The CYLp parameter is highest, when 75 mm/rev feed rate and 13 bar pressure is set, the value is nearly the same with both grain sizes. If the decrease of the peak maximum departure is the goal, it is more advisable to reduce the feed rate: a 3-fold decrease in v_f results in a nearly two-fold decrease.

The valley maximum departure is highest, if 13 bar pressure and 25 mm/rev feed rate are applied with both type of honing tools. Its value is highly affected by the pressure, a nearly two-fold increase in p results in a nearly two-fold increase in the CYLv parameter. The feed rate has a lesser impact, and its effect comes into play on the 13 bar pressure level. Overall, from Figure 4 it can be concluded, that the cylindricity error can be lowered by

reducing the feed rate and the pressure and increasing the grain size. These results in a better abrasive material removal with longer contact time.

The taper and the beforementioned ratio parameters are studied based on Figure 4, which present the surface graphs of Equation 5-7. The first pair of graphs, which are being analysed describes the alteration of the taper. The $CYLt$ value is highest in the analysed range, when 75 mm/rev feed rate and 7 bar pressure is set. The grain size has a low effect on the taper. The increase of the pressure and the decrease of the feed rate have a similar effect; however, it is interesting to note, that if both are changed, no additional effect can be examined.

The $CYLp/CYLt$ and $CYLv/CYLt$ have an opposite alteration characteristic, as it can be expected. Where the former is higher, the latter is lower. According to these graphs, the structure of the cylindricity error can be manipulated by the proper choice of the set parameters. If we increase the feed rate or decrease the pressure before the honing process, the cylindricity will be determined more by the peak maximum departure, and if the alterations of the beforementioned setting parameters are opposite, the cylindricity will be characterized by the valley maximum departure.

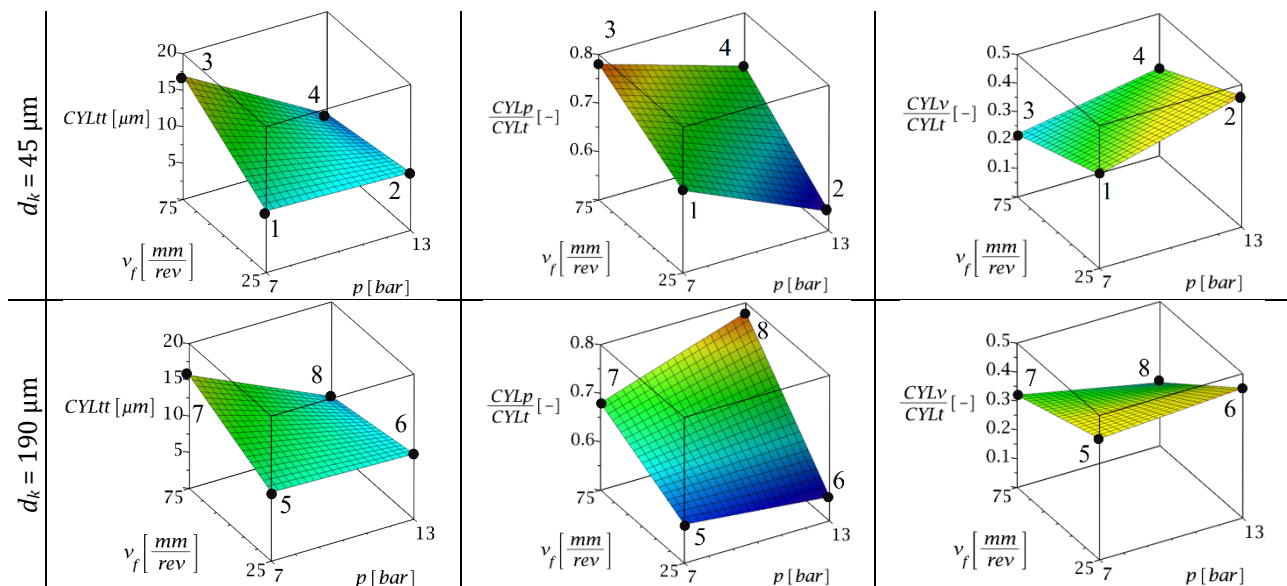


Fig. 4 Alteration of the $CYLt$ and the ratio values in the studied range (the setup numbers are shown)

5. Summary

The study examines cylindricity errors in bore holes created using the honing process, a precision machining technique. The primary objectives are to measure these errors, understand the impact of various honing parameters, and identify optimal conditions for minimizing cylindricity errors. The paper provides valuable insights into the factors affecting cylindricity in bore holes honed by the long-stroke process. The honing experiments are carried out by the application of the full factorial design plan. The effect of the pressure, feed rate and grain size are studied on the cylindricity error, the valley maximum departure, the peak maximum departure and the taper. The carried-out evaluation highlighted the following findings:

- The lowest cylindricity error is achieved by setting the pressure to 7 bar, the feed rate to 25 mm/rev and applying a honing tool with 45 μm grain size.
- Increasing the grain size decreased the overall cylindricity error in the studied range.
- It is advisable to reduce the feed rate and the pressure, but the setup parameters must be carefully chosen.

Acknowledgement

The author fully acknowledged the University of Miskolc for supporting this work.

Conflict of Interest

The author declares that there is no conflict of interests regarding the publication of the paper.

Author Contribution

The author confirms sole responsibility for the following: study conception and design, data collection, analysis and interpretation of results, and manuscript preparation.

References

- [1] Shen, T., & Lu, C. (2023). Assembly accuracy analysis of cylindrical parts based on skin model shapes considering form deviations and local surface deformations. *Precision Engineering*, 80, 256–273. <https://doi.org/10.1016/j.precisioneng.2023.01.004>
- [2] Dawson, D. J. (1992). Cylindricity and its measurement. *International Journal of Machine Tools & Manufacture/International Journal of Machine Tools and Manufacture*, 32(1–2), 247–253. [https://doi.org/10.1016/0890-6955\(92\)90085-u](https://doi.org/10.1016/0890-6955(92)90085-u).
- [3] Engineering Essentials (2024). GD&T - CYLINDRICITY <http://www.engineeringessentials.com/gdt/cylindricity/cylindricity.htm>
- [4] KEYENCE America. (2024). Form Tolerance (Form deviation) | Types of Geometric Tolerances | GD&T Fundamentals | <https://www.keyence.com/ss/products/measure-sys/gd-and-t/type/form-tolerance.jsp#section4>.
- [5] Umarov, T., Turonov, M., & Meliboyev, Y. (2023). Influence of Design and Cutting Conditions On the Accuracy of the Hole Obtained by Drills with Multifaceted Non-Regrind-Able Inserts (MNP). *International Journal of Integrated Engineering*, 15(7), 157-165. <https://doi.org/10.30880/ijie.2023.15.07.015>.
- [6] Motorcu, A. R., & Ekici, E. (2022). Evaluation and multi-criteria optimization of surface roughness, deviation from dimensional accuracy and roundness error in drilling CFRP/Ti6Al4 stacks. *FME Transactions*, 50(3), 441-460.
- [7] Machno, M., Trajer, M., Bizoń, W., & Czeszkiewicz, A. (2022). A study on accuracy of Micro-Holes drilled in TI-6AL-4V alloy by using electrical discharge machining process. *Advances in Sciences and Technology/Postępy Nauki I Techniki*, 16(6), 55–72. <https://doi.org/10.12913/22998624/155224>.
- [8] Felhő, Cs., Tesfom, F., & Varga, Gy. (2023). ANOVA analysis and L9 Taguchi design for examination of flat slide burnishing of unalloyed structural carbon steel. *Journal of Manufacturing and Materials Processing*, 7(4), 136. <https://doi.org/10.3390/jmmp7040136>.
- [9] Varga, Gy., & Ferencsik, V. (2020). Analysis of cylindricity error of high and low temperature storage tested alternator stators. *International Journal of Automotive Technology*, 21(6), 1519–1526. <https://doi.org/10.1007/s12239-020-0143-3>.
- [10] Nagy, A., & Varga, Gy. (2021). Effect of abandonment of cooling and lubrication on surface roughness and cylindricity in turning of steel. *Multidiszciplináris Tudományok*, 11(4), 395–407. <https://doi.org/10.35925/j.multi.2021.4.43>.
- [11] Varga, Gy., Dezső, G., & Szigeti, F. (2022). Shape accuracy Improvement in selective Laser-Melted TI6AL4V cylindrical parts by sliding friction diamond burnishing. *Machines*, 10(10), 949. <https://doi.org/10.3390/machines10100949>.
- [12] Kuti, R., Könczöl, F., Csapó, L., Papp, C., Földi, L., & Tóth, Á. (2024). Selection of engine oils with tribological examinations applicable to specially operated diesel engines. *FME Transactions*, 52(2), 335-342.
- [13] Karpuschewski, B., Pieper, H., Welzel, F., & Risse, K. (2012). Alternative strategies in finishing cylinder running surfaces. *CIRP Annals*, 61(1), 559–562. <https://doi.org/10.1016/j.cirp.2012.03.119>.
- [14] Sadizade, B., Araee, A., Oliaei, S. N. B., & Farshi, V. R. (2020). Plateau honing of a diesel engine cylinder with special topography and reasonable machining time. *Tribology International*, 146, 106204. <https://doi.org/10.1016/j.triboint.2020.106204>.
- [15] Mawandiya, B. K., Sonagara, A., Balar, T., Patel, K. M., & Shah, D. B. (2022). Productivity improvement in honing machining process. *Materials Today: Proceedings*, 59, 283–288. <https://doi.org/10.1016/j.matpr.2021.11.114>.
- [16] Buj-Corral, I., Sender, P., & Luis-Pérez, C. J. (2023). Multi-objective optimization of tool wear, surface roughness, and material removal rate in finishing honing processes using adaptive neural fuzzy inference systems. *Tribology International*, 182, 108354. <https://doi.org/10.1016/j.triboint.2023.108354>.
- [17] Kundrak, J., Fedorovich, V., Pyzhov, I., Ostroverkh, Y., & Pupan, L. (2022). Numerical simulation of grain concentration effect on output indicators of diamond grinding. In *Lecture notes in mechanical engineering* (pp. 165–175). https://doi.org/10.1007/978-3-031-16651-8_16
- [18] Baron, S., Tounsi, T., Gäbler, J., Mahlfeld, G., Stein, C., Höfer, M., Sittinger, V., Hoffmeister, H., Herrmann, C., & Dröder, K. (2022). Diamond coatings for advanced cutting tools in honing and grinding. *Procedia CIRP*, 108, 589–594. <https://doi.org/10.1016/j.procir.2022.03.093>
- [19] Petruš, P., Barényi, I. & Majerík, J. (2023). Microstructure investigation of cast irons with nodular and flake graphite via nanoindentation. *Engineering Review*, 43 (2), 1-7. <https://doi.org/10.30765/er.1861>
- [20] Germann, H., Starke, P., Kerscher, E., & Eifler, D. (2010). Fatigue behaviour and lifetime calculation of the cast irons EN-GJL-250, EN-GJS-600 and EN-GJV-400. *Procedia Engineering*, 2(1), 1087–1094. <https://doi.org/10.1016/j.proeng.2010.03.117>
- [21] Taylor Hobson (2011). *Exploring Roundness - A fundamental guide to the measurement of cylindrical form*. Taylor Hobson Limited. Leicester, England, p. 100